

Oxygen chemisorption on Al: Unoccupied extrinsic surface resonances and site-structure determination by surface soft-x-ray absorption

Antonio Bianconi*

Stanford Synchrotron Radiation Laboratory, Stanford University, Stanford, California 94305

R. Z. Bachrach and S. A. Flodström†

Xerox Palo Alto Research Center, Palo Alto, California 94304

(Received 30 October 1978)

Surface soft-x-ray absorption (SSXA) spectroscopy using synchrotron radiation has been applied to study oxygen chemisorption on aluminum (100), (110), and (111) single-crystal surfaces. Evidence is presented of oxygen-related extrinsic surface resonances above the Fermi level on all faces. From analysis of the SSXA spectra over a large energy range, local structural information has been obtained. The Al (111) surface exhibits a SSXA spectrum dominated by the core transitions to the antibonding states of the Al-O complex in the chemisorption phase. Evidence of a chemisorption phase at oxygen exposures below 50 L has also been obtained for the Al (100) surface. Different charge transfer from Al to O occurs on the two faces, and we suggest the formation of an Al-O complex on the Al(100) with a small charge transfer from Al to O. The transition to the formation of Al₂O₃ has been characterized by the appearance of the oxide core exciton.

I. INTRODUCTION

Understanding the initial interaction of oxygen with aluminum surfaces has been of considerable experimental¹⁻⁹ and theoretical¹⁰⁻¹³ interest. The research has focused on occupied bonding levels and core line shifts. Evidence of a chemisorption phase on the Al(111) face was found where single-bonded oxygen is outside the surface.⁵ This model is in agreement with experimental data concerning photoemission,²⁻⁵ work function,⁸ and plasmon coupling with core lines.⁹ The chemisorption phase on the (111) face is characterized by a 1.4-eV chemically shifted Al**-2p* core line resulting from a smaller charge transfer from Al to the chemisorbed oxygen than that of the Al³⁺ *2p* in the oxide (2.8 eV). In spite of theoretical investigations suggesting the existence of oxygen chemisorbed outside the Al(100) surface, little experimental evidence has been accumulated. Most work on the (100) face has been interpreted in an island growth model where bulklike oxide nuclei are first formed at surface active sites. However, for very low exposures, less than 50L (1 langmuir = 10⁻⁶ Torr sec), where no Al-*2p* chemical-shift peak is observed^{4,6} and the work function does not change as a function of oxygen exposure,⁸ the nature of the Al-O interaction is not clear. Early LEED data suggest that an ordered O overlayer does form on this face.¹⁴

In this paper we present results which provide new information concerning the electronic bonding and the local site structure of oxygen chemisorption and the evolution to an oxide on aluminum (100), (110), and (111) single-crystal faces. The

photoyield technique has been used to study the aluminum unoccupied density of states and the electronic antibonding states of the Al-O complexes formed during the initial oxygen chemisorption on aluminum. We have recently shown^{15,16} that the photoyield technique can be used to measure surface soft-x-ray absorption spectra with high surface contrast.

Surface soft-x-ray absorption cross section (SSXA) has been measured by using the photoyield or constant-final-state photoemission technique with the final-state energy (E^*) tuned to coincide with the valence-band (VB) interatomic Auger transition Al-*2p*-O-*2s* at 45 eV. (The details of these transitions are discussed in Sec. III A.) The surface $L_{2,3}$ photoabsorption cross section is measured by recording the intensity as a function of the exciting-photon energy of the Auger electrons which result from the nonradiative recombination of the Al-*2p* core hole created by the absorption event. The high final-state energy used in this work provides advantages over the more conventional low-energy final state used in partial-yield spectroscopy tuned to secondary electrons.^{17,18} First, the electron effective escape depth $l(E^*)$ is a minimum, thus providing better surface contrast. In fact, $l(E^*)$ of 45-eV electrons is about 2 Å in aluminum.¹⁹ Second, the measurement is better tuned to those Al atoms interacting with the chemisorbed oxygen. With this technique it is possible to measure the $L_{2,3}$ spectrum over a 50-eV energy range free of direct photoemission peaks.¹⁵ Soft-x-ray absorption spectroscopy (SXA) has grown rapidly in the last ten years by using synchrotron radiation. SXA is a sensitive probe of

the local structure around the absorbing atom.²⁰ This spectroscopy concerns the electronic transitions from a localized atomic core level to unoccupied excited states with surface sensitivity established by the short electron escape depth. The main contribution to the matrix element of the core transitions comes from the local character of the initial-state wave function overlapping the final state. A molecular description of the final-state wave function is often found to be sufficient to interpret the spectra near the edge. This aspect of the spectroscopy is very attractive for studying adsorbates on solid surfaces since one is interested in the local interaction with the substrate, and molecular-like bonds are very important.

In agreement with other spectroscopies, our measurements show differences in oxygen chemisorption on the three low-index surfaces.³⁻⁷ The results summarized here are presented in detail in Secs. III C–III E and discussed in Secs. IV B–IV E. On the (111) surface, a SSXA spectrum typical of the chemisorption phase⁵ is found which is nearly invariant with the oxygen exposure up to the onset of oxide formation. The formation of the oxide is easily recognized by the appearance of the excitonic “inner-well state”¹⁵ on the spectrum which remains invariant up to 10^6 L, characteristic of the thin layer oxide.^{15,16} In the chemisorption phase, a new unoccupied oxygen-related extrinsic surface resonance has been found at 85 eV. In this energy range, an intrinsic surface resonance is observed on the clean Al(111) surface. With oxygen chemisorption the resonance shifts toward higher energy, forming an extrinsic resonance. An extrinsic resonance is also found on the Al(100) surface at 84.7 eV. The spectral feature becomes sharper and stronger than the weak structure at 84 eV on the clean surface which corresponds to an empty surface state in a partial gap along the $X-M$ direction of the surface Brillouin zone at 10.5 eV above E_F .²² The strong intrinsic surface resonance at 4.3 eV above Fermi level²² disappears with oxygen exposure. Our results clearly confirm the formation of a chemisorbed oxygen monolayer outside the metal surface at exposures less than 100 L on the Al(111) surface. On the Al(100) surface the oxide formation is observed above 50 L. These data suggest that oxygen is also chemisorbed for very low exposure on this face, but with a small charge transfer from Al so that no chemically shifted Al-2*p* core line is observed. A similar chemisorption state has been recently observed²³ on the Si(111) 2×1 surface. A model of oxygen “covalently” bonded to the silicon surface has been proposed.²³

II. EXPERIMENTAL

The experiment was performed on the 4° beam line²⁴ at the Stanford Synchrotron Radiation Laboratory using monochromatized synchrotron radiation emitted by the storage ring SPEAR. The samples were oriented high-purity electrochemically polished single crystals of aluminum.²⁵ Transmission electron microscopy showed an almost perfect (111) surface, a very good (100) surface having some defects, and a (110) surface displaying a large amount of faceting and other surface defects. The initial surface was cleaned *in situ* by successive argon sputtering at 300 °C and then annealed at 400 °C for 0.5 h at a pressure of 2×10^{-10} Torr. Cleanliness was checked by Auger-electron spectroscopy and valence-band photoemission spectroscopy using 50-eV photons to increase the surface sensitivity. Only the (110) face showed residual oxygen corresponding to approximately 0.5-L exposure. Low-energy electron diffraction (LEED) analysis showed good surface order after the final annealing. Incoming *p*-polarized light illuminated the sample at 5°–10° from grazing incidence. The final-state kinetic energy of the electrons was selected with a double-pass cylindrical mirror analyzer. The surface soft-x-ray absorption spectra (SSXA) were measured with the constant-final-state photoemission technique. The technique consists in measuring the number of electrons emitted, $N(E^* = \text{const.}, \hbar\omega)$, at a fixed kinetic energy as a function of the photon energy. The electron analyzer detects a cone at $\theta = 42^\circ$ so that only Auger electrons $E^* = 45$ eV coming from an average 2.9-Å layer [$2 l(E^*) \cos\theta$] contribute to the measured spectrum. In Fig. 1 a scheme of the experimental apparatus is shown. The resolution of the SSXA spectra is determined by the

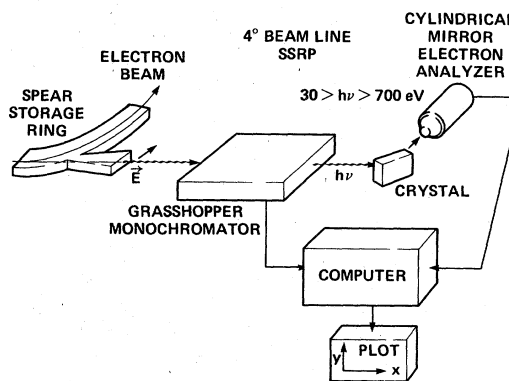


FIG. 1. Experimental apparatus used to measure the SSXA spectra by the constant-final-state photoemission technique on the 4° beam line at the Stanford Synchrotron Radiation Laboratory.

monochromator resolution, which is about 0.1 eV at 100 eV and varies as $(\hbar\omega)^2$. All the SSXA spectra were normalized to the incoming photon flux, which was measured using a photomultiplier with a sodium salicylate converter. Data acquisition and handling were done by a computer (PDP 11/40) connected on line. The clean Al surface at a base pressure of 2×10^{-10} Torr was exposed to molecular oxygen statically introduced in the vacuum chamber. The sample was exposed to 1-L O_2 or less at a gas pressure of 10^{-8} Torr followed by consecutive exposures of 10 L at 10^{-7} Torr. Pressures of 10^{-6} Torr were used for the 100-L and higher exposures. The data have been taken over a year in different runs and good reproducibility of the results, following similar procedures of the oxygen exposure, has been found.

III. RESULTS

A. Interatomic Auger recombination

The interatomic Auger recombination of the $L_{2,3}$ hole is plotted in Fig. 2, which shows $N(E, \hbar\omega = \text{const.})$, the electron energy distribution curves (EDC) of an aluminum (111) surface at several oxygen exposures (1 langmuir = 10^{-6} Torr sec). The lower curve shows the spectrum of clean aluminum using a photon excitation energy $\hbar\omega = 77$ eV which is just above the $L_{2,3}$ threshold at 72.72

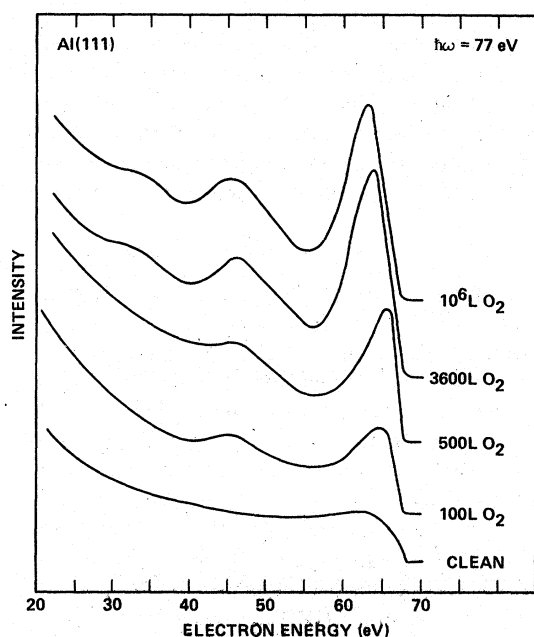


FIG. 2. Electron EDC excited by 77-eV photons for clean aluminum and at several oxygen exposures (1 L = 10^{-6} Torr sec).

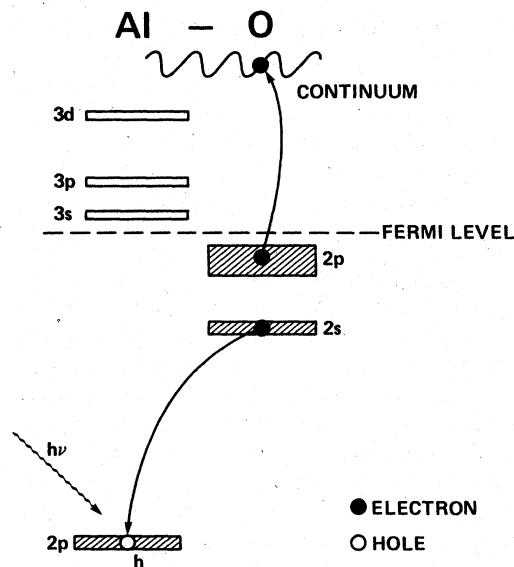


FIG. 3. Schematic picture of the interatomic Auger recombination of the Al-2p core hole followed by the emission of a 45-eV electron in the continuum.

eV. When one uses photons with enough energy to create a hole only in the 2p core level, the spectrum of the Auger-electron transitions is simpler than the Auger spectrum excited by high-energy electrons.⁸ The peak at 63 eV corresponds to the $L_{2,3}VV$ Auger transition of aluminum metal.²⁶ After oxygen exposure, this peak changes and a new peak induced by oxygen chemisorption appears at 45 eV. We have assigned the peak at 45 eV to an interatomic Auger transition since its energy does not depend on the photon energy and it is close to the Al-2p-O-2s core-level separation of 50.5 eV.²⁷ The electronic transition O-2s-Al-2p was observed at $\hbar\omega = 50.5$ eV by Fomichev²⁸ in x-ray fluorescence spectra. Since the aluminum work function is ≈ 4.3 eV, one would expect the Al-2p-O-2s VB interatomic Auger transition to be below 46.2 eV. The peak at 45 eV is the only Auger peak below 46.3 appearing with oxygen chemisorption, so the assignment is unambiguous. Figure 3 shows a schematic picture of the interatomic Auger process. To measure the SSXA spectra we have recorded the intensity of this interatomic Auger peak as a function of the photon energy. We have called this technique interatomic Auger yield spectroscopy (IAYS) to distinguish it from the conventional partial-yield spectroscopy (PYS), where one is collecting only secondary electrons. The improved surface sensitivity of our technique¹⁵ is at least as good as that obtainable with electron-energy-loss spectroscopy (ELS)²⁹ using low-energy electrons (typically 100 eV), but with

energy resolution better than that of ELS. Moreover, ELS generally measures derivative spectra so the shape of the absorption peaks, like excitons and resonances, which is important in the interpretation of the spectra, cannot be recorded.

B. SSXA of the clean crystal surfaces

Figure 4 shows the $L_{2,3}$ SSXA spectra of the Al(111) and Al(100) clean surfaces together with the bulk SXA spectrum measured by optical transmission measurements of an aluminum polycrystalline film evaporated *in situ*. Surface resonances on the clean surface have been identified in the SSXA spectra at ~ 77 eV and at ~ 85 eV.²² These features are not present in the bulk spectrum which is flat and structureless up to about 10 eV above the $L_{2,3}$ edge. Another aspect is the extended x-ray absorption fine structure (EXAFS) modulations above 90 eV which shift toward higher energies in the Al(111) spectrum. In the bulk spectrum,³⁰ the peak at 97 eV and the minimum at 104 eV in Fig. 4 correspond to the first large EXAFS modulation of the photoabsorption cross section due to final-state interference effects produced by atoms around the absorbing one. From the analysis of the surface EXAFS structures in the

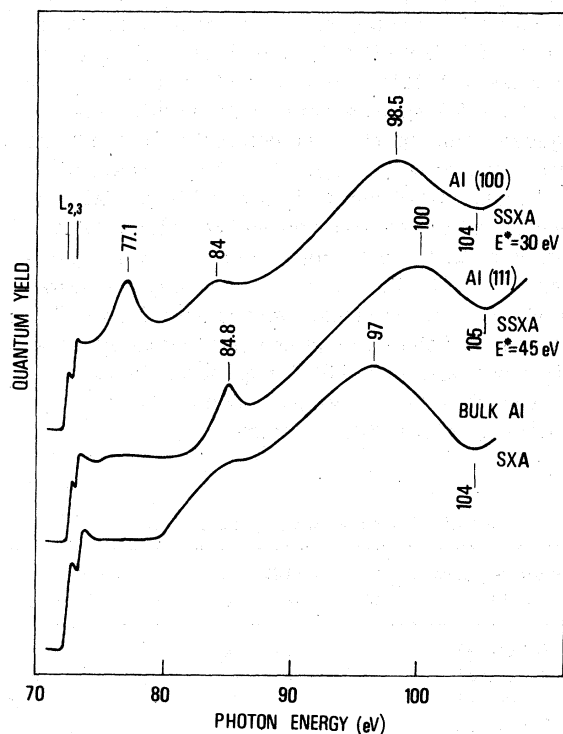


FIG. 4. SSXA spectra of the Al(111) and Al(100) surfaces compared in the lower part of the figure with the bulk SXA spectrum of a thick aluminum film.

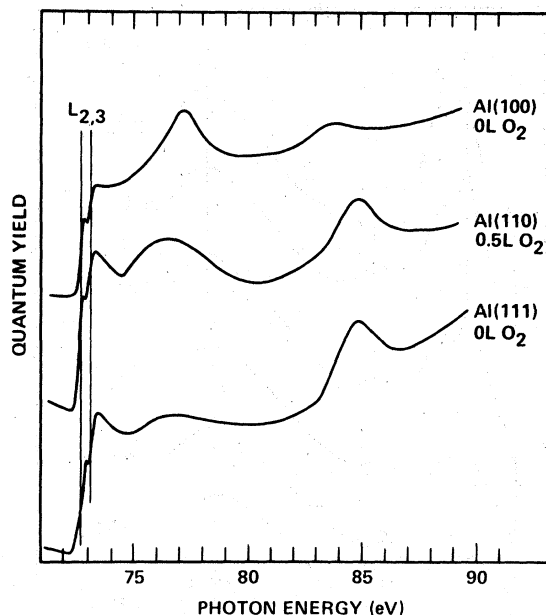


FIG. 5. SSXA of the three low-index crystal surfaces near the $L_{2,3}$ threshold, in the energy range dominated by the intrinsic surface resonances.

SSXA spectra, we have found³¹ a contraction of the spacing between the first two surface layers $\Delta d = 0.19 \pm 0.05 \text{ \AA}$ on the Al(111) surface and no relaxation on the Al(100) surface. Figure 5 shows the SSXA spectra of the clean crystal surfaces in the energy range of unoccupied surface resonances. The (110) had some residual oxygen corresponding to 0.5 L of oxygen. Therefore the observed structures are partially induced by oxygen chemisorption. The intensity and the energy of the unoccupied resonances is clearly face dependent, as is also found for the occupied surface resonances.⁴

C. Oxygen chemisorption on the (111) surface

Figure 6 shows the SSXA spectra of the Al(111) surface at several oxygen exposures. At only 0.4-L- O_2 exposure one can observe the typical features of the chemisorption phase.⁵ These features remain unchanged up to above 100 L. With respect to the clean spectrum, the peaks D and E shift toward higher energy and a broad band appears with the threshold T_1 at 74.4 eV extending up to 81 eV. These structures are superimposed on the aluminum $L_{2,3}$ spectrum which shows the characteristic spin-orbit split $L_{2,3}$ threshold at 72.72 and 73.15 eV. Figure 7 shows the SSXA spectra near the $L_{2,3}$ edge in more detail. At 10 L, two weak oxygen-induced structures S_1 and S_2 can be clearly seen. All the oxygen-induced structures are due to transitions to the antibonding Al-O

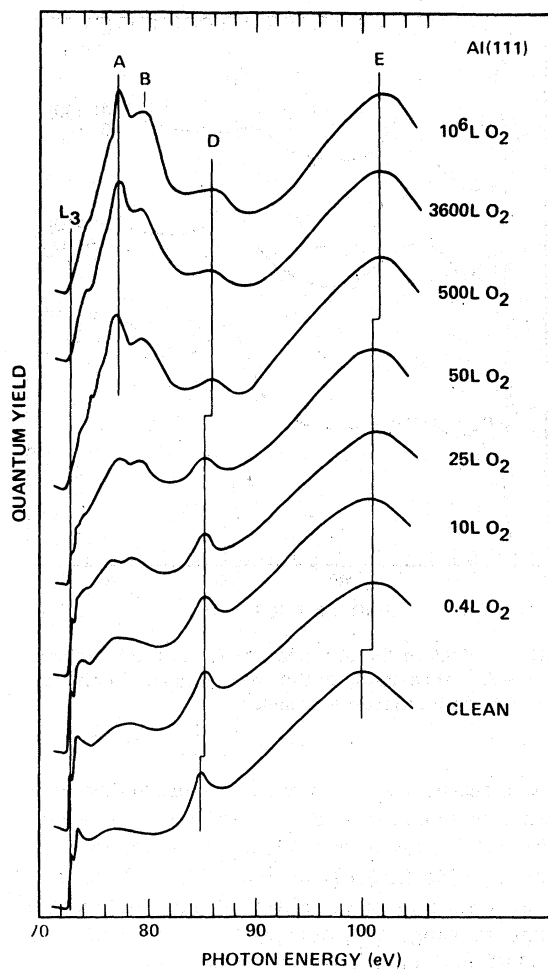


FIG. 6. SSXA spectra of the Al(111) surface at several oxygen exposures.

levels. Since core transitions are a sensitive probe of the local structure,²¹ our data indicate the formation of a stable microscopic structure of the oxygen chemisorbed on the surface, i.e., of the "surface molecule" from a few chemisorbed oxygen atoms to monolayer formation at ≈ 100 L. Above 50 L, in agreement with core-level photoemission data,^{4,5} some oxide clusters are formed as indicated by the appearance of the weak structures corresponding to the "inner well resonances"²¹ *A* and *B* of the oxide. Above 500 L, the SSXA spectra show the transition from the chemisorption phase to the oxide phase and the characteristic features of the oxide spectrum appear. The strong new excitonic peak *A* and the structure *B* typical of the Al_2O_3 $L_{2,3}$ spectrum¹⁵ arise. They are above the threshold T_0 of the transition from the Al^{3+} $2p$ level of the oxide, which is expected at -76.3 eV.¹⁵ The binding energy of the Al^{3+} $2p$ level

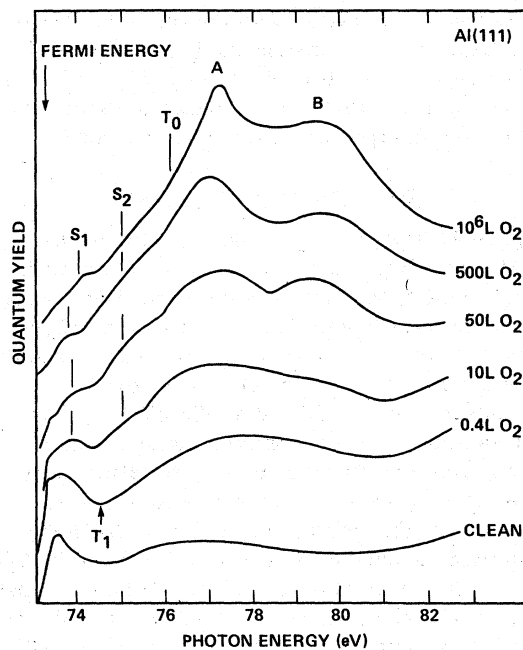


FIG. 7. SSXA spectra near the $L_{2,3}$ threshold of the Al(111) surface at several oxygen exposures.

is 75.8 eV below the Fermi level.³⁻⁵ In the oxide SSXA spectra, the peak *D* broadens, decreases, and shifts toward higher energy at the same time as peak *E*. From the first oxide formation up to about the 5-Å-thick oxide layer¹⁶ formed at 10^6 -L O_2 , the SSXA spectra remain essentially unchanged. The spectra are dominated by the "inner-well resonances" *A*, *B*, *D*, *E* of the microscopic structural unit of the oxide formed by the Al^{3+} ion surrounded by the electronegative O ions. These data show that two stable Al-O configurations appear on the (111) surface, one corresponding to the chemisorption phase, with O outside the Al surface, and the other corresponding to the oxidation phase, above 500-L exposure. In Table I are reported the energy positions of the main structures of the SSXA spectra.

TABLE I. Energies of spectral features.

Oxygen exposure (L)	Al(111)		Al(100)			
	0	50	10 ⁶	0	5	2 × 10 ³
$S_1 \pm 0.3$ eV		73.8	74			73.7
$S_2 \pm 0.3$ eV		75	75			75
$A \pm 0.1$ eV			76.9			76.9
$B \pm 0.2$ eV			79.5			79
$D \pm 0.2$ eV	84.8	85	86	84	84.7	85.4
$E \pm 0.5$ eV	100	100.7	101.5	98.5	99.5	101.5

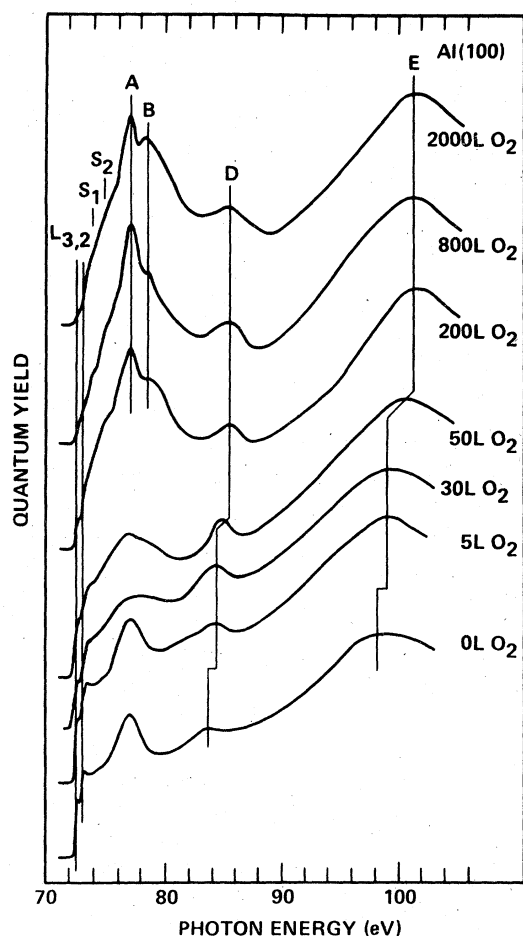


FIG. 8. SSXA spectra of the Al(100) surface at several oxygen exposures.

D. Oxygen chemisorption on the (100) surface

Figure 8 shows the SSXA spectra of the Al(100) surface at several oxygen exposures. The clean surface and the nearly completely oxide-covered surface are, respectively, at the bottom and the top of the figure. The SSXA spectrum typical of the oxide is observed above 50-L-O₂ exposure. The peaks A and B being as strong as the peak E characterize this spectrum. The oxide spectrum is similar to that formed at higher oxygen exposures on the Al(111) surface. The strong peak in the clean spectrum at 4.3 eV above the L_{2,3} threshold, due to a core transition to unoccupied surface state, broadens and decreases with oxygen exposure and at 50 L nearly disappears. The structures D and E of the clean spectrum shift by 0.7 and 1 eV, respectively, toward higher energy. The shift which appears at the lowest exposure we have performed (1 L) remains unchanged

up to 30 L. This indicates that the final states, i.e., the antibonding Al-O levels, do not change in this range of exposures to molecular oxygen. The characteristic threshold T₁ at 74.4 eV of the SSXA spectra of the chemisorption phase on the (111) surface is not observed on the (100) surface. Since this threshold has been associated with the intermediate oxidation state of aluminum, characterized by the 1.4-eV chemically shifted Al* 2p level, our results are in agreement with Ref. 4, where no similar intermediate shift has been found on the (100) surface exposed to oxygen following the same procedure as in this work. Figure 9 shows the SSXA spectra near the L_{2,3} edge for a better display of these features. Before the oxide formation occurs, a broad weak band also appears between the L_{2,3} edge and about 80 eV, corresponding to the similar band on the (111) surface. The SSXA spectrum at 50-L exposure shows an intermediate shift of the peaks D and E since some oxide clusters start to appear on the surface at this exposure.⁴ Below this exposure, the oxygen-induced features are typical of a chemisorption phase of oxygen. In Table I, the energy of the structures of the SSXA spectra at 5- and 2000-L exposures, characteristic of the chemisorption and oxide phase, respectively, are presented.

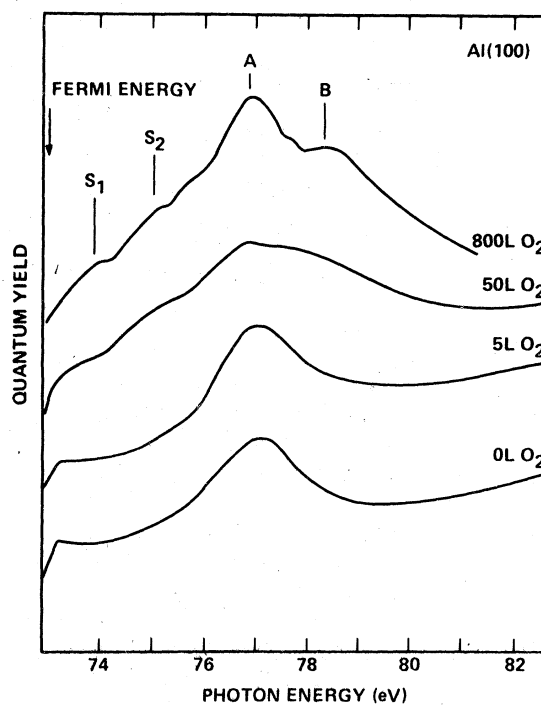


FIG. 9. SSXA spectra near the L_{2,3} threshold of the Al(100) surface at several oxygen exposures.

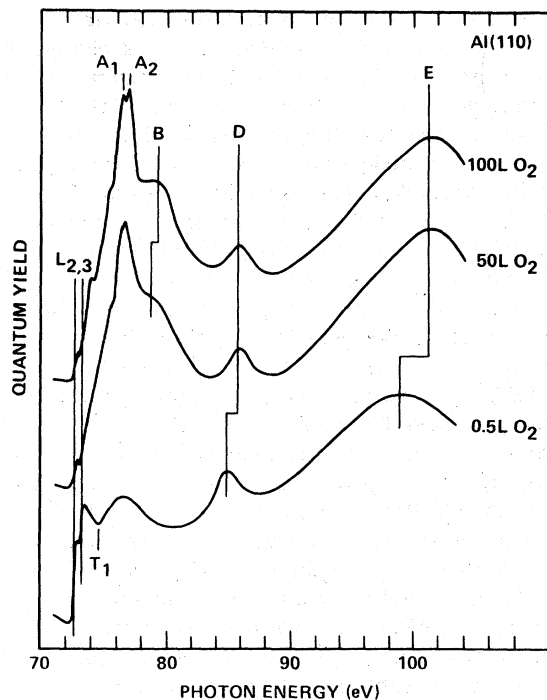


FIG. 10. SSXA spectra of the Al(110) surface at several oxygen exposures.

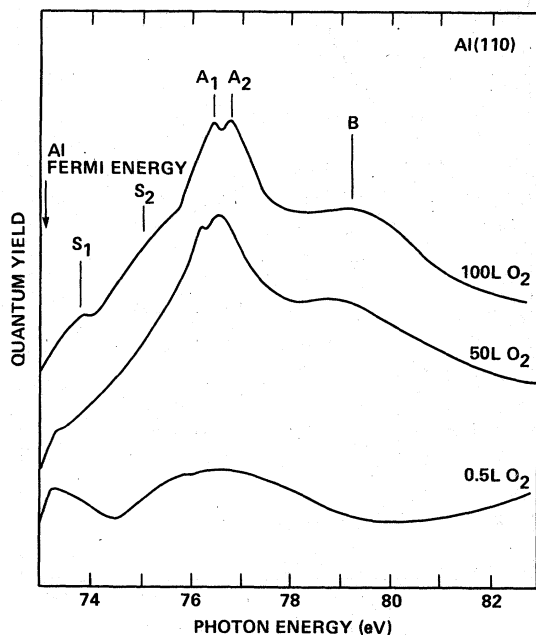


FIG. 11. SSXA spectra near the $L_{2,3}$ threshold at several oxygen exposures of the Al(110) surface.

E. Oxygen chemisorption on the (110) surface

Figure 10 shows the SSXA spectra of the (110) surface at several exposures. The strong peaks *A* and *B* appear at lower exposures than in the other surfaces studied. This indicates faster oxide formation than on the other surfaces. The oxide spectra are similar to the spectra of the thin oxide layer formed on the other surfaces, but the peak *A* is split as in γ -alumina.¹⁵ The cleanest surface has a residual oxygen corresponding to 0.5-L oxygen exposure. The features of the SSXA spectrum of the surface at this exposure are similar to that of the chemisorption phase on the (111) face. The characteristic threshold T_1 of the core transitions from the Al $2p$ level are observed. Figure 11 shows the spectra near the $L_{2,3}$ edge with more detail. The interface transitions S_1 and S_2 (see Ref. 16) are present in the oxide spectra below the threshold of the core transitions from the $Al^{3+} 2p$ level at 76 eV.

IV. DISCUSSION

A. Clean surfaces: resonances and structure

Although bulk aluminum is a free-electron-like metal, its surface behavior shows effects due to localized charge. Filled surface states and resonances have been found on the single-crystal surfaces^{4, 32, 33} by photoemission spectroscopy. We have found also unoccupied intrinsic surface resonances above the Fermi level.²² Peaks in the SSXA spectra are expected for localized final states. In band-structure language, the final states should correspond to critical points of the Brillouin zone where $\nabla_k E(k) = 0$, i.e., to maxima of the joint density of states of the transitions from a core level. On Al(100), the surface resonances at 4.3 eV above the $L_{2,3}$ threshold correspond to core transitions to final states in partial gaps in the surface projected bands,^{22, 34} while for the (111) surface no gaps corresponding to the observed unoccupied surface resonances have been found. Structural information on the Al surfaces were obtained by LEED⁵ and were extracted from SSXA spectra by the analysis of surface extended x-ray absorption fine structures³¹ (SEXAFS). SEXAFS shows a contraction of the interatomic distance between the first surface layer atoms and the underlying atoms by $\Delta r = 0.15 \pm 0.05 \text{ \AA}$ on the (111) and no appreciable contraction on the (100) surface. The LEED data on the (111) face indicate no surface-structure reconstruction following oxygen chemisorption. Further theoretical calculation, based on all these experimental results, will be necessary to clarify the electronic properties of Al surfaces.

B. Oxygen chemisorption on the (111) surface

The first step of oxygen interaction with the Al(111) surface is the formation of an oxygen monolayer chemisorbed outside the surface.⁵ In this phase, a charge transfer from Al to O is revealed by the 1.4-eV chemically shifted Al* 2*p* level. We have identified the extrinsic surface resonances due to core transitions to the antibonding Al-O orbitals in this configuration. The local symmetry, the nature, and the electronegativity of atoms surrounding the one absorbing determines the shape of the soft-x-ray absorption spectra. Within about 20 eV of the $L_{2,3}$ edge, transitions to molecular excited states of the molecular Al-O complex, i.e., of the microscopic structural unit of the chemisorption phase, dominate the spectrum. The experimental evidence that the oxygen-induced structures do not change from 0.4 L up to the monolayer formation at 100 L shows that only the short-range order is important to determine the main features of the SSXA spectra. To interpret the SSXA spectra of this face, the transitions from the two initial states Al* 2*p* and Al 2*p* have to be considered; these contribute to the spectrum for the surface with chemisorbed oxygen exposures of less than 1500 L. The threshold T_1 in Fig. 8 of the transitions from the Al* 2*p* level is expected and observed at the 74.4-eV binding energy of the Al* 2*p* level below the Al Fermi level. The coincidence with the expected value indicates that no gap opens up in the Al-O bonding and antibonding levels in the chemisorption phase and the first allowed oxygen-induced states are just above the Fermi level. The lack of any sharp excitonlike line at this energy gives evidence of an oxygen chemisorption site outside the metal surface.¹⁵ In fact, the core hole created should be screened by the metal free-electron Fermi sea. The broad oxygen-induced resonance between T_1 and 81 eV in Fig. 7 is assigned to Al- sp_3 -O-2*p* antibonding final states. The main contribution of the antibonding states comes from the Al orbitals as shown by theoretical calculations.¹³ This consideration and the oxygen-induced symmetry mixing explain why the extrinsic resonance *D* in the SSXA spectrum of the chemisorption phase is strongly related to the intrinsic resonance *D* which shifts and broadens with oxygen chemisorption. The structure S_1 below T_1 threshold cannot be assigned to a transition from the Al ion inner shell in the intermediate oxidation state and therefore it should be assigned to an interatomic transition from the Al 2*p* level of the metal to the antibonding states of the Al-O complex. Extension of the theoretical calculations¹³ to unoccupied states of the chemisorption phase of

oxygen on the (111) surface using either the energy band¹³ or cluster¹¹ approaches, when compared with our experimental data, should give new information on the microscopic bonding.

The SSXA spectra of the thin oxide layer are characterized by the "inner-well states" *A*, *B*, *E* of the Al₂O₃ molecular units.^{15,16} The excitonic transition *A* to the Al (*s*-like) final state is associated with the existence of the ionized Al³⁺ ion completely surrounded by electronegative oxygen ions. The oxygen ions should be incorporated in the metal to form a molecular Al₂O₃ unit and to insulate the 2*p* hole from the metal conduction electrons to allow the existence of this core exciton or discrete inner-well state.^{15,16}

C. Oxygen chemisorption on the (100) surface

The chemisorption of oxygen on the Al(100) surface has been the object of several theoretical investigations.^{11,13} The first approach is the "surface molecule" cluster model in which an atom or molecule at the surface and a limited number of near-neighbor substrate atoms form a molecular cluster.¹¹ The second approach is based on an energy-band model^{12,13} in which two-dimensional periodicity of the adsorbate on the surface plane is assumed. Chemisorption of O outside the metal surface has been proposed.¹¹⁻¹³ Photoemission experiments show that the Al³⁺-2*p* core-level shift corresponding to an oxide appears above 50-L-O₂ exposure without the appearance of a smaller "chemisorption" shift as is observed on the (111) face,^{3,4} and therefore do not show the presence of a chemisorbed phase. The SSXA spectra of this face confirms the photoemission result since the characteristic threshold T_1 of the transition from the core level of the Al ion in the intermediate oxidation state is not observed but also indicates the presence of a chemisorbed phase. The data of Gartland⁸ indicate that an island oxide growth mechanism characterizes the 100 surface. Below 50-L exposure, no chemically shifted Al-2*p* peak was observed if oxygen is chemisorbed, although the valence band shows the O-2*p* resonance band at -7.4 eV below the Fermi energy. This would indicate little charge transfer from metal to oxygen site. We suggest that in the Al-O interaction on the (100) face, the charge can be removed from the occupied surface state observed on the clean surface^{4,32,33} and a chemisorption phase also exists on this surface for exposures at low pressure below 50 L. For higher exposures, we agree with the island oxide growth model.^{4,8} The work function data are in agreement with our results since they do not show any change below 50 L.⁸

The *A* peak characteristic of the molecular Al₂O₃

cluster formation appears only above 50 L. The oxygen chemisorption removes the intrinsic surface resonance at 4.3 eV above the edge. The core transitions to the antibonding Al-O levels just above the Fermi level form a weak broad band extending up to 7 eV above the edge similar to the band observed on the (111) chemisorption phase. The extrinsic surface resonance D at 84.7 eV becomes stronger and is shifted toward higher energies in comparison with the corresponding intrinsic resonance. This different trend with oxygen chemisorption of this resonance in comparison with the D resonance on the (111) face is clearly related to the different "surface molecule" on the two surfaces with oxygen chemisorbed outside the surface. The final state of this transition can be associated with the highest flat band near the X_4 critical point of the band-structure calculation of the two-layer Al(100) film with a 1×1 oxygen overlayer in hole centered configuration (see Fig. 3 of Ref. 13) calculated by Painter.¹³ The aluminum orbitals contribution to this final state should be quite large, and the interaction with the O orbitals modifies and shifts these conduction bands of the surface with chemisorbed oxygen.

D. Oxygen chemisorption on the (110) surface

This surface shows faster reactivity with oxygen to form oxide. This very open surface exhibits at 50-L exposure practically only oxygen on the surface. The 0.5-L spectrum, however, suggests that also on this surface a chemisorption

phase is possible. The large similarity of this spectrum with the spectrum of the chemisorption phase on the (111) face indicates the existence of the intermediate oxidation state of Al ions interacting with oxygen. Further studies will be necessary to better understand the chemisorption on this surface.

V. SUMMARY

New aspects of the oxidation of the (100), (110), and (111) single-crystal faces have been revealed using surface-soft-x-ray absorption spectroscopy. The presence of oxygen-related extrinsic surface resonances above the Fermi level on all three faces has been shown. The initial interaction of oxygen has been shown to proceed by a chemisorption phase on all three faces, but with different charge-transfer aspects. The transition to the formation of Al_2O_3 has been characterized by the appearance of the oxide core exciton.

ACKNOWLEDGMENTS

The authors are grateful to H. Winick and the staff of the Stanford Synchrotron Radiation Laboratory for their support during the experiment. Thanks are due to J. C. McMenamin, M. Hecht, and H. A. Six for help with the measurements. Some of the material incorporated in this work was developed with the financial support of the NSF (under Contract No. DMR7727489) (in cooperation with the Department of Energy).

*Present address: Instituto di Fisica, Università di Roma, Roma, Italy, and PULS Laboratori Nazionali di Frascati, Frascati, Italy.

†Dept. of Physics, University of Linköping, Sweden.

¹K. Y. Yu, J. N. Miller, W. E. Spicer, N. D. Lang, and A. R. Williams, *Phys. Rev. B* **15**, 1446 (1976).

²S. A. Flodstrom, R. Z. Bachrach, R. S. Bauer, and S. B. M. Hagstrom, *Phys. Rev. Lett.* **37**, 1282 (1976).

³S. A. Flodstrom, R. Z. Bachrach, R. S. Bauer, and S. B. M. Hagstrom, *Proceedings of the Seventh International Vacuum Congress and International Conference on Solid Surfaces*, edited by R. Dobrozensky (F. Berger and Sohne, Vienna, 1977), p. 869.

⁴R. Z. Bachrach, S. A. Flodstrom, R. S. Bauer, S. B. M. Hagstrom, and D. J. Chadi, *J. Vac. Sci. Technol.* **15**, 488 (1978).

⁵S. A. Flodstrom, C. W. B. Martisson, R. Z. Bachrach, S. B. M. Hagstrom, and R. S. Bauer, *Phys. Rev. Lett.* **40**, 907 (1978).

⁶W. Eberhardt and C. Kunz, *Surf. Sci.* **75**, 709 (1978).

⁷D. Norman and D. P. Woodruff, Daresbury report D1/SRF/P109 (unpublished).

⁸P. O. Gartland, *Surf. Sci.* **62**, 183 (1977).

⁹A. M. Bradshaw, W. Domcke, and L. S. Cederbaum, *Phys. Rev. B* **16**, 1480 (1977).

¹⁰N. D. Lang and A. R. Williams, *Phys. Rev. Lett.* **34**, 531 (1975).

¹¹J. Harris and G. S. Painter, *Phys. Rev. Lett.* **36**, 51 (1976).

¹²I. P. Batra and S. Ciraci, *Phys. Rev. Lett.* **39**, 774 (1977).

¹³R. P. Messmer and D. R. Salahub, *Phys. Rev. B* **16**, 3415 (1977); and G. S. Painter, *Phys. Rev. B* **17**, 662 (1978).

¹⁴S. M. Bedair, F. Hofmann, and H. P. Smith, Jr., *J. Appl. Phys.* **39**, 4016 (1968).

¹⁵A. Bianconi, R. Z. Bachrach, and S. A. Flodstrom, *Solid State Commun.* **24**, 539 (1977).

¹⁶A. Bianconi, R. Z. Bachrach, S. B. M. Hagstrom, and S. A. Flodstrom, *Phys. Rev. B* **19**, 2837 (1979).

¹⁷D. E. Eastman and J. L. Freeouf, *Phys. Rev. Lett.* **33**, 1601 (1974); J. L. Freeouf and D. E. Eastman, *Crit. Rev. Solid State Sci.* **5**, 245 (1975).

¹⁸W. Gudat and D. E. Eastman, *Photoemission from Surfaces*, edited by B. Feuerbacher, B. Fitton, and R. F. Willis (Wiley, London, 1977), Chap. 11.

¹⁹C. J. Powell, R. J. Stien, P. B. Needham, Jr., and T. J. Driscoll, *Phys. Rev. B* **16**, 1370 (1977).

²⁰F. C. Brown, *Solid State Phys.* **29**, 1 (1974).

²¹J. L. Dehmer, *J. Chem. Phys.* **56**, 4496 (1972).

- ²²R. Z. Bachrach, D. J. Chadi, and A. Bianconi, *Solid State Commun.* **28**, 931 (1978).
- ²³C. M. Garner, I. Lindau, C. Y. Su, P. Pianetta, J. N. Miller, and W. E. Spicer, *Phys. Rev. Lett.* **40**, 403 (1978).
- ²⁴F. C. Brown, R. Z. Bachrach, and N. Lien, *Nucl. Instrum. Methods* **152**, 73 (1978).
- ²⁵Crystals were supplied by Materials Research Corp. USA and published by P. O. Gartland, Norway; see J. K. Grepstad and P. O. Gartland, *Surf. Sci.* **57**, 348 (1976).
- ²⁶C. J. Powell, *Phys. Rev. Lett.* **30**, 1179 (1973).
- ²⁷A. Balzarotti and A. Bianconi, *Phys. Status Solidi B* **76**, 683 (1976).
- ²⁸V. A. Fomichev, *Sov. Phys. Solid State* **8**, 2312 (1967).
- ²⁹J. E. Rowe, *Solid State Commun.* **15**, 1505 (1974); R. Ludeke and L. Esaki, *Phys. Rev. Lett.* **33**, 653 (1974).
- ³⁰T. M. Hayes and P. N. Sen, *Phys. Rev. Lett.* **33**, 653 (1975).
- ³¹A. Bianconi and R. Z. Bachrach, *Phys. Rev. Lett.* **42**, 104 (1979).
- ³²P. O. Gartland and B. J. Slagsvold, *Solid State Commun.* **25**, 489 (1978).
- ³³G. V. Hannon and S. A. Flodstrom, *Phys. Rev. B* **18**, 1562 (1978).
- ³⁴E. Caruthers, L. Kleinman, and G. P. Alldredge, *Phys. Rev. B* **8**, 4570 (1973); **9**, 3330 (1974).